Towards ultraviolet optoelectronic systems on silicon substrates

Mike Cooke reports on III–nitride semiconductor on silicon technologies enabling photonic on-chip data transfer and improved material quality for higher-efficiency photon emission and detection.

Crystal nitrides of metals from the group-III column of the Periodic Table of elements — aluminium (AlN), gallium (GaN) and indium (InN) — exhibit conduction-valence bandgaps covering the range of near- and mid-ultraviolet (UV) photon energies from 3.1eV up to 6.2eV with corresponding limit wavelengths of 400nm and 200nm.

Electron transitions between the conduction and valence bands can hence emit and detect UV radiation in these ranges and the production of functioning devices on various substrates have been demonstrated for over 20 years, and have resulted in commercial applications.
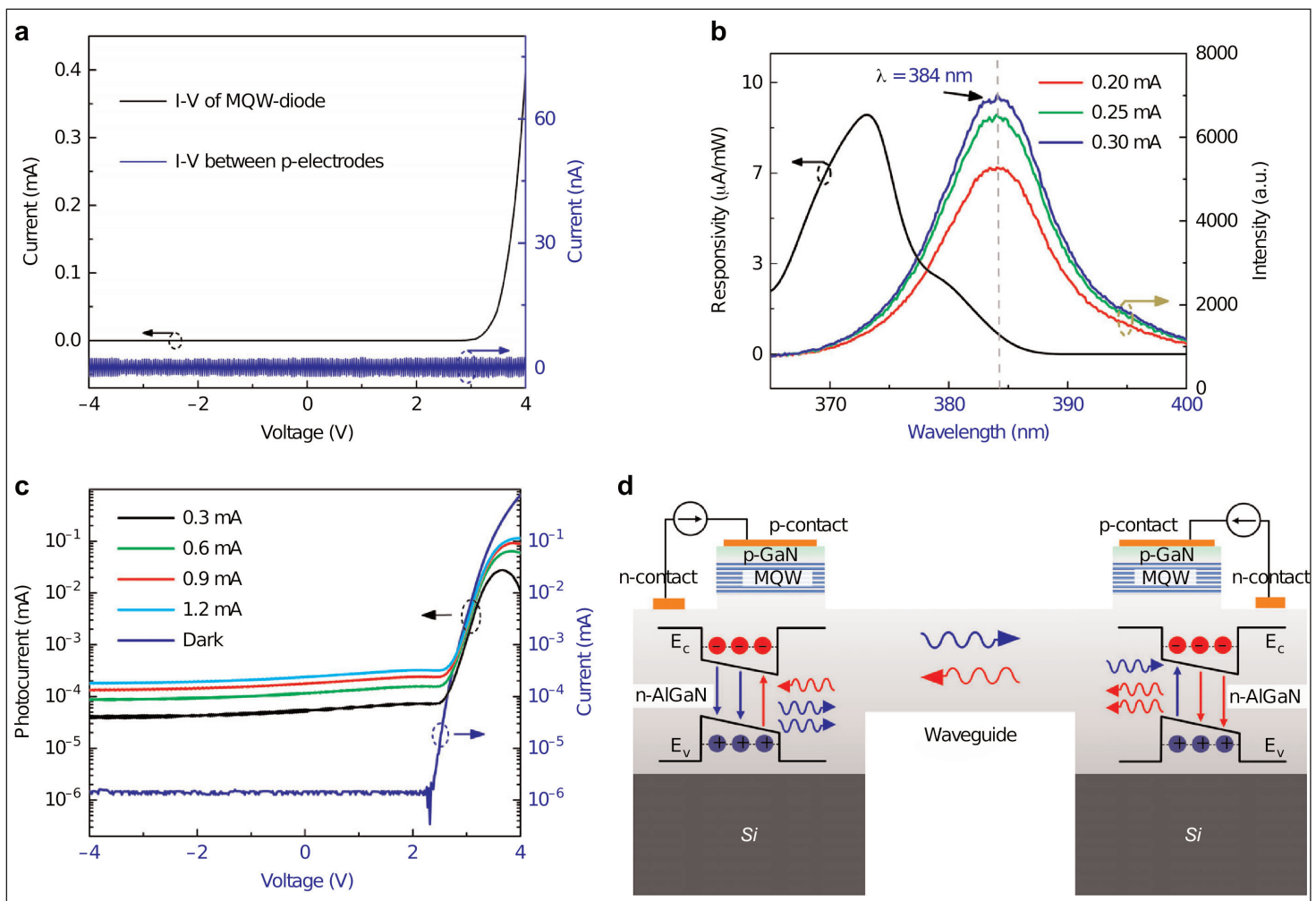

Figure 1. Optical & electrical performance of monolithic multi-component system. (a) Measured current–voltage I–V curves. (b) Electroluminescence spectra and spectral responsivity of ring MQW-diode. (c) Induced photocurrent at circular MQW-diode as function of injection current of ring MQW-diode. (d) Schematic of full-duplex light communication of monolithic multi-component system using identical MQW-diodes.

Growth on silicon, rather than much more expensive sapphire or silicon carbide (SiC), would significantly reduce production costs. Also, silicon is available in larger-diameter formats for mass production. Another advantage of silicon is potential integration with smart driving and signal-processing circuitry based on mainstream CMOS electronics.

The drawback of growth on silicon is lower-quality material that reduces device efficiency. In particular, epitaxial AlGaN layers are generally strained due to lattice-constant (~19%) and thermal expansion (~50%) mismatching with silicon. Strain is relieved by the generation of defects and dislocation structures in the atomic lattice that form efficiency-sapping leakage paths and non-radiative recombination centers. More efficient UV-emitting devices, enabled by improved material quality, would enhance performance and cost effectiveness of laser printing, high-capacity data storage, white lighting, water purification and sterilization.

Here we report on attempts to use III–N semiconductor on silicon technology for on-chip optical data transfer, more efficient photo-detection, and to improve material quality for UV light-emitting diodes (LEDs).

Monolithic systems

Nanjing University of Posts and Telecommunications in China has been working on monolithic near-UV optoelectronic combinations of InGaN multiple quantum well (MQW) diodes connected by waveguides on silicon [Yongjin Wang et al, Light: Science & Applications, vol7, p83, 2018]. The diode devices were able to both generate and detect light signals encoding an audio stream in a real-time full-duplex set up. This builds on work reported earlier this year in collaboration with Nagoya University in Japan [Chuan Qin et al, Appl. Phys. Express, vol11, p051201, 2018; reported in Mike Cooke, Semiconductor Today, p96, May/June 2018].

The researchers comment: "The self-generated photocurrent opposes a change in the injection current that produced it, indicating that self-absorption may be associated with the efficiency droop phenomenon of light-emitting diodes under high-injection conditions." On the application side, they see "great potential for diverse applications, such as UV sensing, curing, sterilization, and on-chip power monitoring" from monolithic multi-component systems.

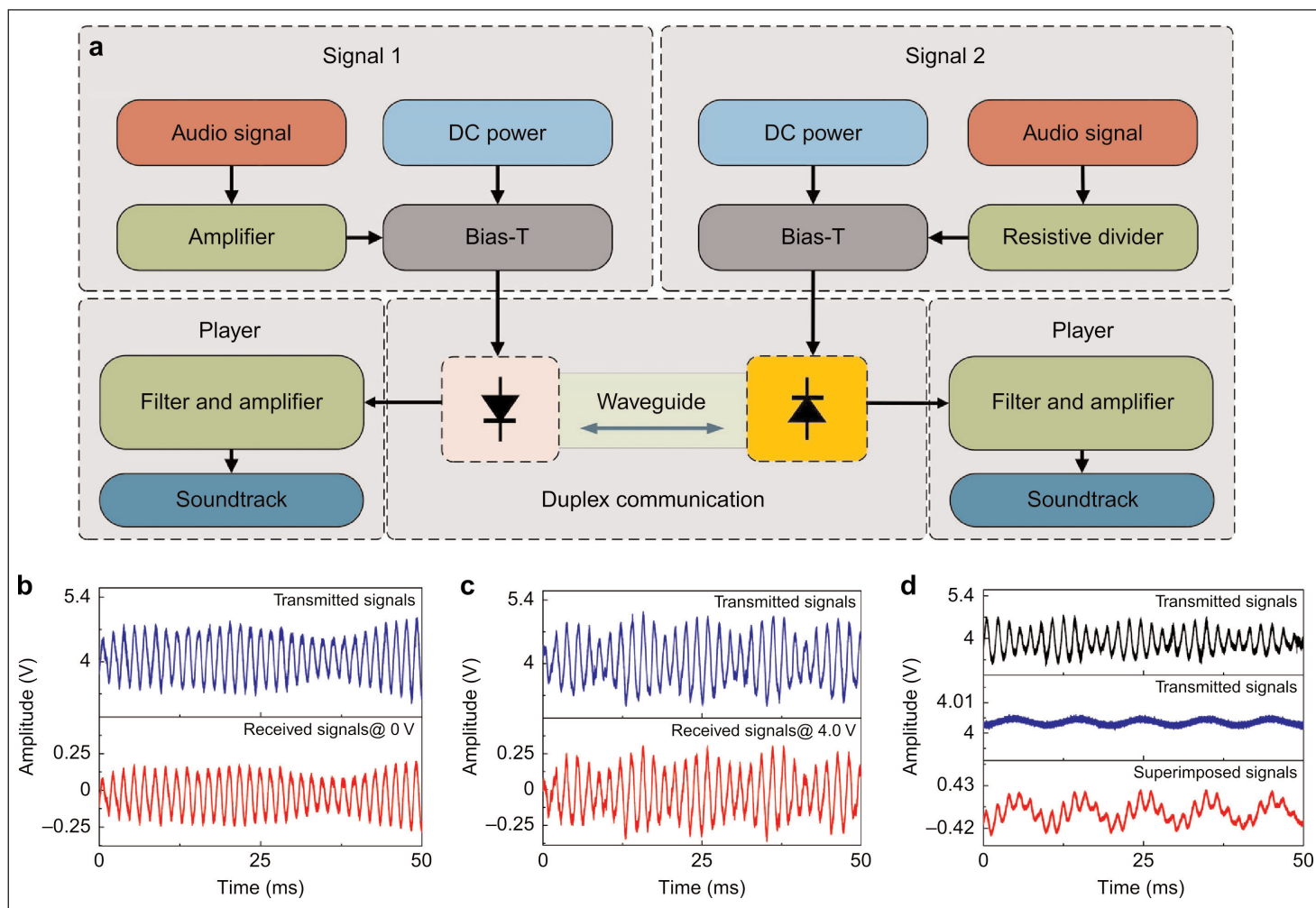A buffer of step-graded aluminium nitride (AlN) and

Figure 2. Full-duplex audio communication using monolithic multi-component system. (a) Schematic. (b) Audio signals received at circular MQW-diode with zero bias. (c) Audio signals received at circular MQW-diode with bias voltage of 4.0V. (d) Superimposed signals under simultaneous emission-detection condition.
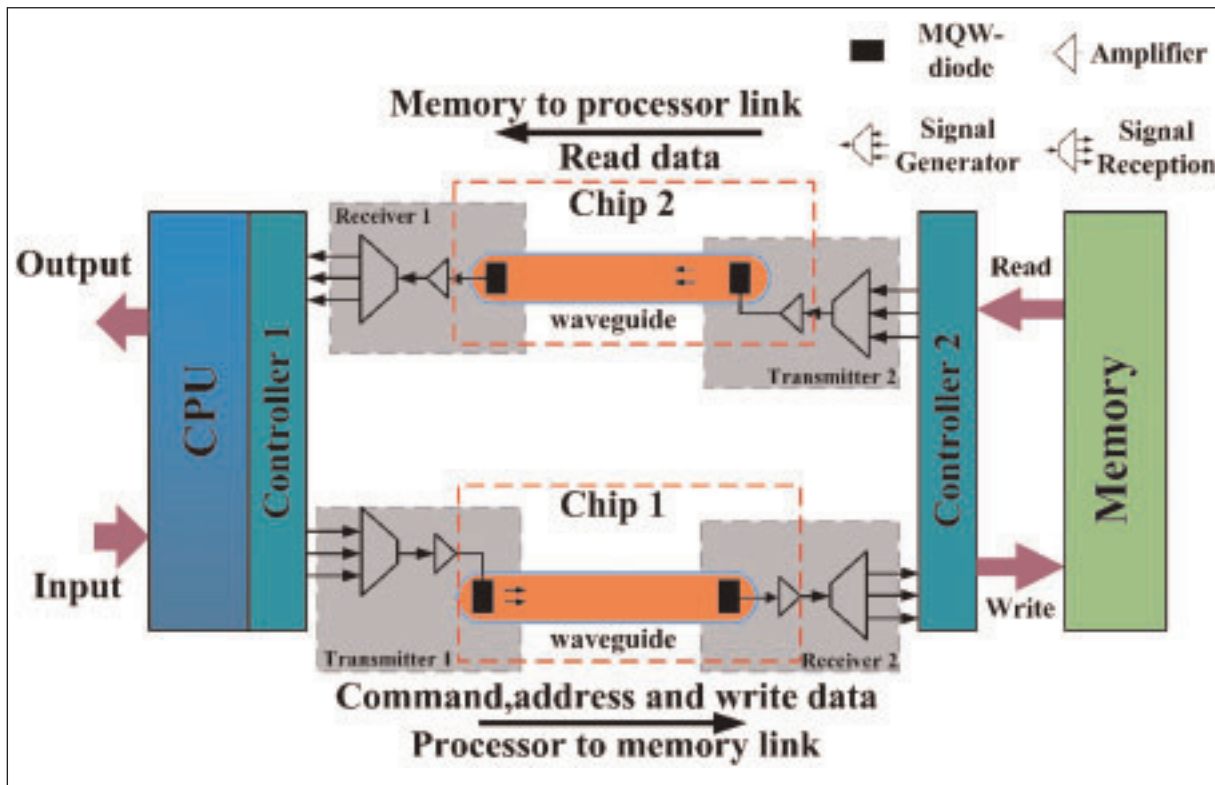
Figure 3. Schematic of optical communication between processor and memory via monolithic multi-component system.

aluminium gallium nitride (AlGaN) layers was grown on (111) Si. Then, a thick n-$Al_{0.05}Ga_{0.95}N$ layer was followed by a superlattice of 30 pairs of $In_{0.02}Ga_{0.98}N$/$Al_{0.10}Ga_{0.90}N$. The active light-emitting region consisted of five InGaN QWs separated by $Al_{0.10}Ga_{0.90}N$ barriers. The indium content of the 3nm-thick wells is described as "low". The p-side of the device was completed with 80nm p-$Al_{0.05}Ga_{0.95}N$ and 10nm p-GaN contact.
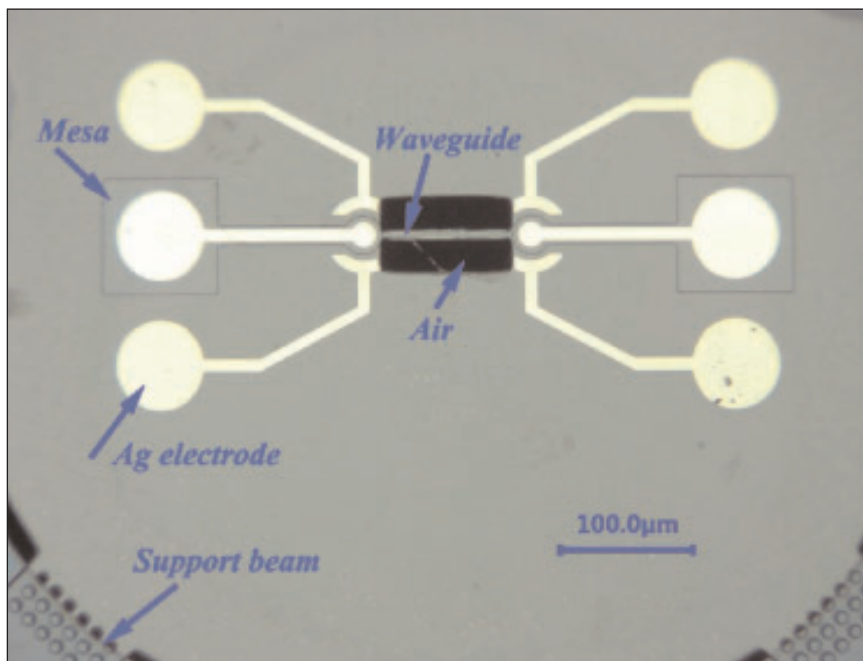
The material was fabricated into two diode devices connected by a 8μm-wide 130μm-long suspended waveguide. The p-electrodes were circular with 120μm diameter. One of the electrodes was of ring form to allow the devices to be distinguished for easy identification. The n- and p-electrodes were nickel/silver. The large difference in refractive index between the III–nitride material and air confined the light to the plane of the waveguide. The waveguide suspension was achieved by locally removing the silicon substrate using back-side etching. Without the silicon removal, the light would be heavily absorbed across the III–N/silicon interface. The refractive index of silicon is in fact higher than that of III–N materials.

The ring diode had a turn-on voltage of 3.0V, emitting radiation with a dominant peak around 384nm (Figure 1). Removal of the silicon substrate from under the diode shifted the emission wavelength due to changes in the stress built into the material. The researchers found a 40nm overlap of the wavelengths of the emission spectrum and response spectrum of the circular (non-ring) detecting diode.

The researchers used the devices to achieve full-duplex audio communication — i.e. each device was simultaneously a transmitter and receiver (Figure 2). The bias voltage was 4.0V and there was additional driving circuitry to enable encoding and decoding of the signals.

The researchers have also used the technology for microprocessor-memory communication [Yongjin Wang, Appl. Phys. Express, vol11, p122201, 2018]. The optical links enabled microprocessor read/write from/to memory operations (Figure 3). The suspended waveguides were 8μm wide and 100μm long.

Figure 4. Optical microscopy image of monolithic multi-component system.

The researchers linked two ATmega328 chips with one of the chips sending read/write instructions to the other's 2kbyte SRAM at a rate of 1200 baud, using two separate optical links for the read and write functions.

The team also carried out experiments towards merging the two optical links into one (Figure 4). The 'transmitter' and 'receiver' were variously biased and modulated at megahertz speeds. The team plans to code the phase of the separate signals for two-way signal transfer: "Using the self-interference cancellation method, the received signals are obtained by subtracting the transmitted signals from the superimposed signals." There is also an expected trade-off where the modulation rate increases with decreasing electrode size.

Microwire arrays

South China Normal University and Peking University in China have developed UV metal-semiconductor-metal (MSM) detectors based on GaN microwire arrays on (100) silicon [Dexiao Guo et al, ACS Photonics, published online 1 November 2018]. The researchers claim superior performance compared with most reported GaN nano/microwire- or thin-film-based UV detectors. The team sees application potential for future photoelectronic and on-chip optoelectronic integrated systems. The (100) orientation of silicon is preferred for high-speed and low-power CMOS electronics.

The researchers used a top-down technique for creating horizontal microwires that should enable better repeatability in manufacturing compared with bottom-up growth methods that suffer from random placement, and uneven diameter or curvatures, of vertical wires. Further, the technique avoids the need for complicated lift-off and layer transfer of structures to another substrate or other complex processes that increase production costs.

The 2-inch high-resistivity (100) silicon substrate was prepared with a 300nm plasma-enhanced chemical
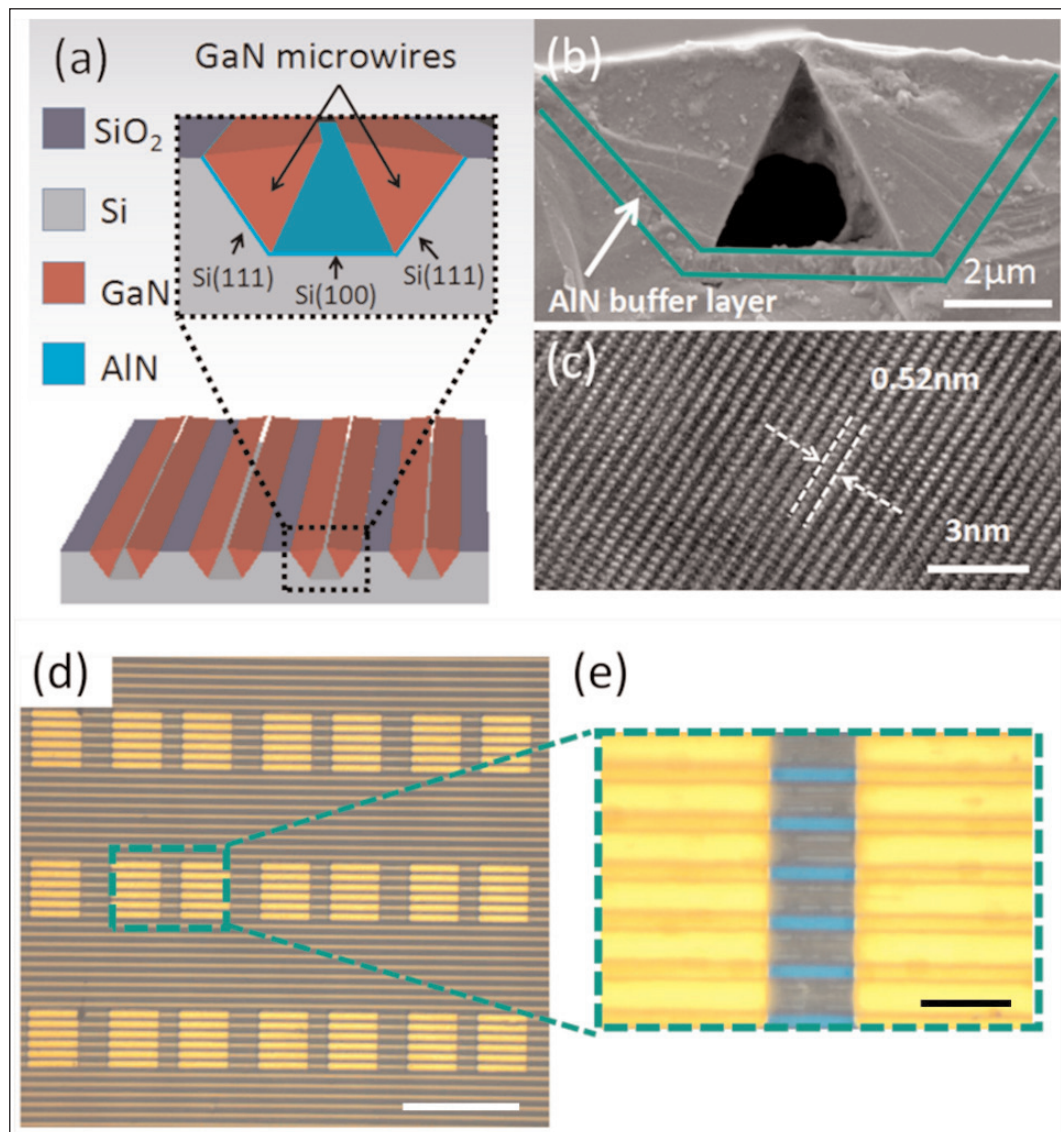

Figure 5. (a) Schematic of GaN-based microwire arrays on patterned silicon substrate. (b) Typical scanning electron microscope image. (c) High-resolution transmission electron microscope image of GaN microwire. (d) Optical microscope image of fabricated orderly arranged detectors; scale bar 100μm. (e) Enlarged image of one detector; scale bar 20μm.

vapor deposition (PECVD) silicon dioxide layer that was patterned into 3μm stripes separated by 7μm silicon gaps. Potassium hydroxide wet etching of the silicon created trapezoidal channels with (111) facets that present a hexagonal atomic arrangement most conducive to III–nitride growth. Native oxide was then removed with hydrofluoric acid solution.

The microwire arrays were produced with low-pressure (100mbar) metal-organic chemical vapor deposition (MOCVD) of 300nm AlN insulating buffer and then unintentionally doped GaN (Figure 5). The wires were contacted with two patterned nickel/gold Schottky electrodes 20μm apart. Photoluminescence experiments (Figure 6) showed a sharp and high-intensity near-band-edge emission peak centered at 364.5nm (~3.4 eV). Yellow luminescence, which indicates impurities and defects, was not observed.
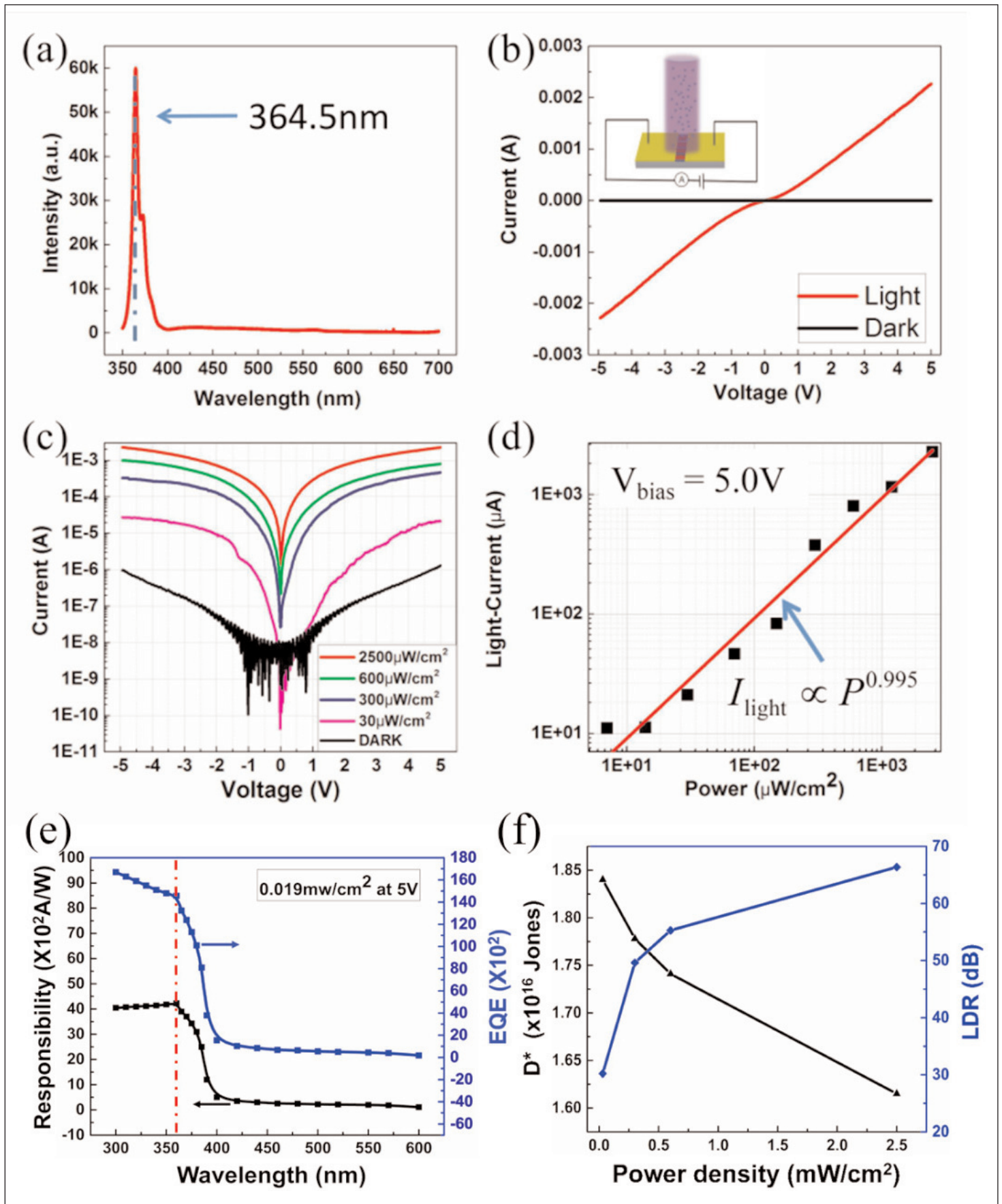
Figure 6. (a) Room-temperature micro-photoluminescence spectrum of GaN microwire. (b) Current–voltage characteristics both in dark (black curve) and under 325nm UV illumination (red curve); inset, testing schematic diagram of photodetector. (c) Light-density-dependent current-voltage curves. (d) Current variation as function of light intensity. (e) Responsivity and EQE-dependent wavelength curves. (f) Specific-detectivity-dependent power density curves.

With 5.0V bias under 2500µW/cm^2 325nm helium-cadmium laser power, the current was 2.71mA. Dark current was 1.3µA, giving a sensitivity of 2.08x10^5%. The current-light output power dependence followed a power law with exponent 0.995. The exponent being close to 1 indicates a low density of trap states and high crystal quality of the GaN microwires. The responsivity was calculated at 1.17x10^{5}A/W, while the external quantum efficiency (EQE) came in at 4.47x10^5. The maximum specific detectivity was 10^{16}Jones.

The researchers claim that their UV photodetector performs in terms of high sensitivity, high responsivity and high EQE, much better than most reported single GaN nano/microwire- and nanowire-array-based photodetectors.

The team's device also improves on most reported GaN-based alternatives in terms of a turn-on time of 36.3ms under 2500µW/cm^2 illumination. During reset, there were two exponential processes — a fast one of 75.2ms, followed by a much more extended decay of 9.66s. The researchers suggest traps or other defect states could be involved in the persistent photoconductivity after turn-off of the light source. The researchers suspect that oxygen is desorbed from the surface during UV illumination. When reabsorbed, the oxygen traps electrons, delaying the full return to the dark current state.

The team also created a comparison device on sapphire with 3µm GaN layer. The devices featured nickel/gold contacts. The electrode lithography used the same photomask as for the microwire device on silicon. The sensitivity, responsivity and EQE were 2.77x10^4%, 0.21A/W and 0.80, respectively.

Lateral epitaxial overgrowth

Researchers based in Japan, USA and Turkey have developed technology for high-brightness UV AlGaN LEDs using material grown on 200mm silicon substrates [Yoann Robin et al, Materials Science in Semiconductor Processing, vol90, p87, 2019]. The team from Japan's Nagoya University, Virginia Commonwealth University in the USA, Turkey's Cumhuriyet University and Northwestern University in the USA used lateral epitaxial overgrowth methods to improve material quality. The researchers report: "Improvement of the AlN quality and the structure design allowed the optical output power to reach the milliwatt range under pulsed current, exceeding the previously reported maximum efficiency."

The UV-emitting material was grown on (111) silicon using metal-organic chemical vapor deposition. First, a 120nm seed layer of AlN was grown and then patterned for lateral epitaxial overgrowth. The patterning consisted of 2µm-deep trenches along the [10$\bar{1}$0] direction of the AlN structure ([11$\bar{2}$] relative to silicon substrate). The trenching resulted in stripes that were 2µm wide with 4µm period.

Further AlN buffer growth was performed at high temperature with precursors delivered in hydrogen carrier gas in pulses. The growth of AlN on the seed stripes coalesced after about 6µm of growth. The AlN
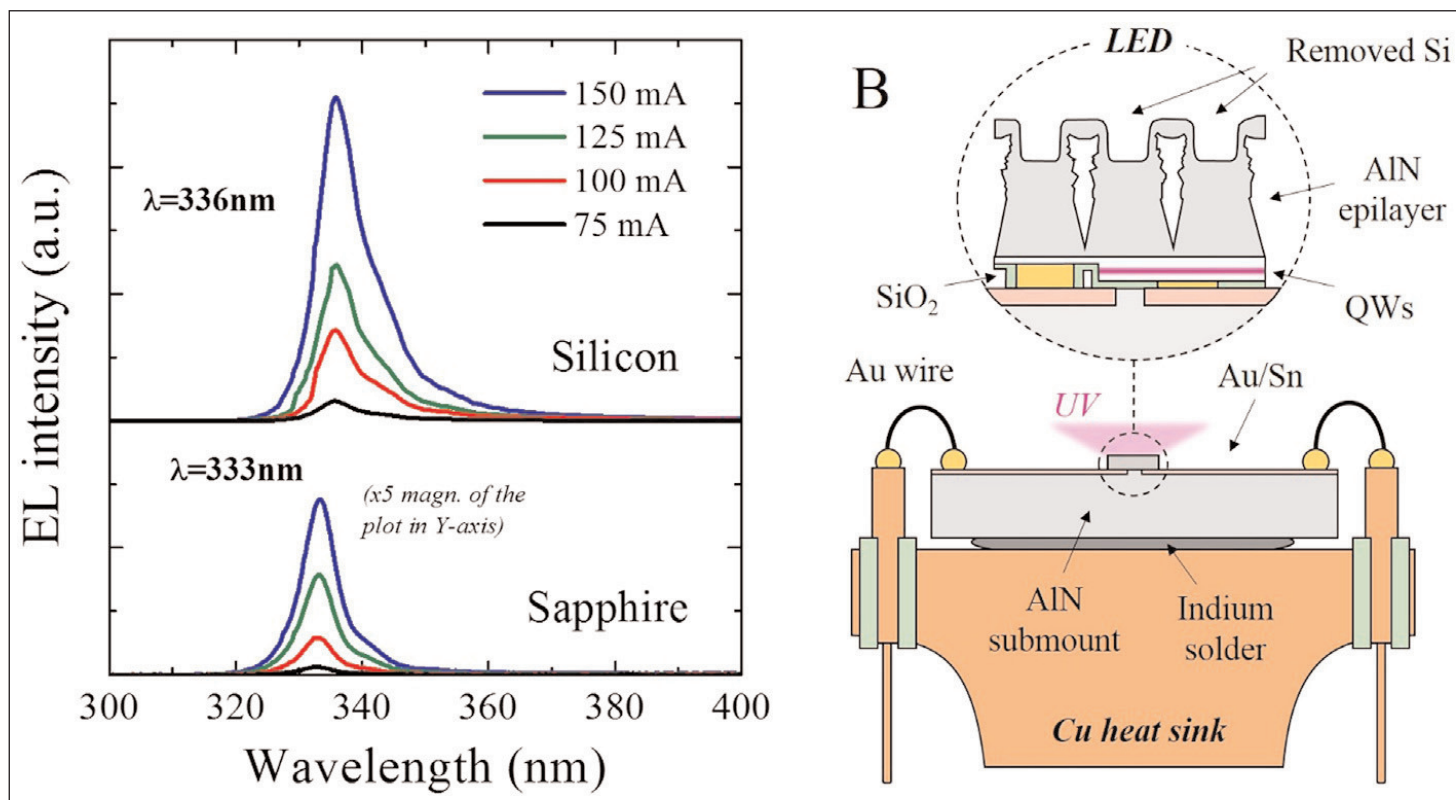

Figure 7. (A) Electroluminescence spectra of UV-LEDs grown on silicon and sapphire (Al$_2$O$_3$) recorded at different current densities. (B) Schematic of device structure grown on silicon.
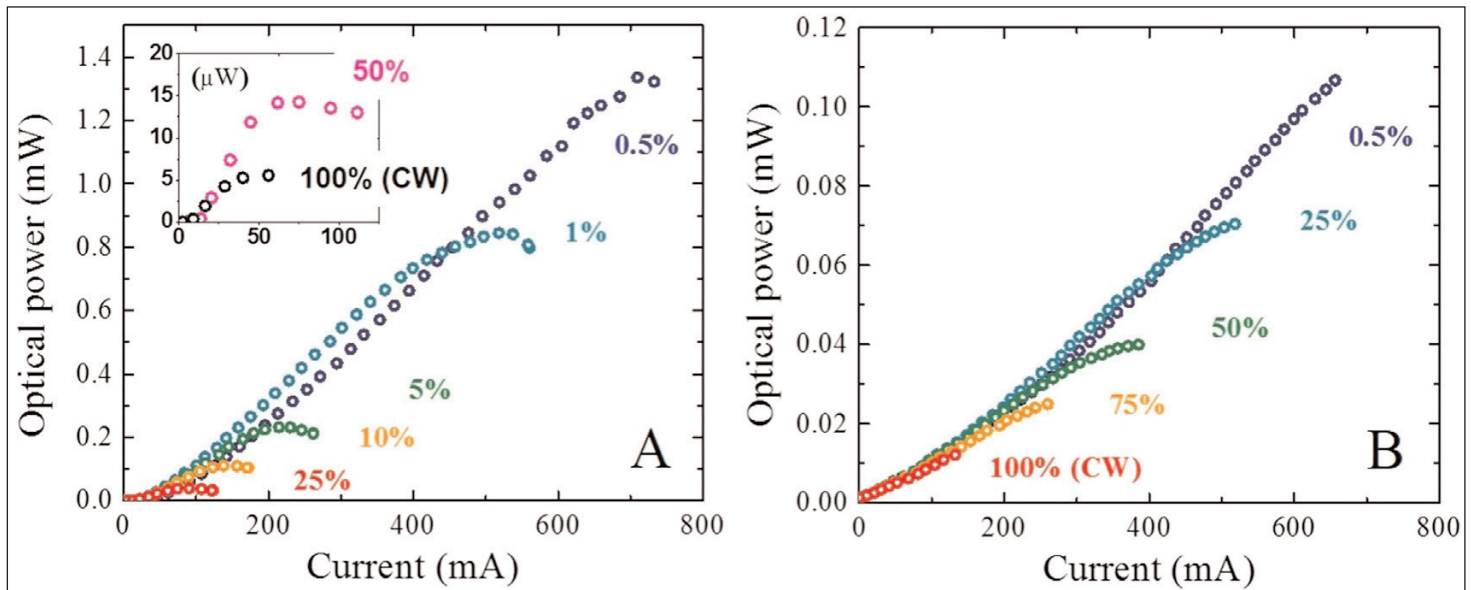
Figure 8. Optical output power measurements of UV-LEDs grown on silicon (A) and sapphire (B) as a function of injection current for different duty cycles.

template was used as the base for growth of 600nm of silicon-doped n-$Al_{0.2}Ga_{0.8}N$, five 3nm $Al_{0.05}Ga_{0.95}N$ wells separated by 7nm $Al_{0.15}Ga_{0.85}N$ barrier layers, a 10nm magnesium-doped p-$Al_{0.3}Ga_{0.7}N$ electron-blocking layer, 100nm of magnesium-doped p-$Al_{0.15}Ga_{0.85}N$ and 50nm of magnesium-doped p-GaN. A comparison epitaxy of the same AlGaN structure was carried out on a 350nm AlN buffer on polished c-plane sapphire.

LED fabrication began with rapid thermal annealing (RTA) to activate the magnesium doping of the p-type layers. The 300μmx300μm device mesas were defined by electron cyclotron resonance (ECR) reactive ion etch. Nickel/gold and titanium/gold were deposited by electron-beam evaporation as the p- and n-type electrodes, respectively. Silicon dioxide was used for passivation. Further metalization added a thick titanium/gold layer that made contact with both electrode types.

The LED chips were flipped and mounted on pre-patterned AlN submounts with gold-tin eutectic bonding. The silicon substrate was removed using a hydrofluoric/nitric/acetic acid mix. The sides of the devices were protected with wax during the wet etching. Substrate removal is vital since silicon strongly absorbs UV radiation, unlike sapphire. The devices were then bonded to copper heat-sinks with indium, and finally wire bonds were made for electrical connection. The comparison sapphire-based LED was fabricated similarly, but without substrate removal.

The devices emitted a narrow peak around 336nm wavelength in 1%-duty-cycle pulsed operation (10μs period); the comparison LEDs grown on sapphire emitted nearby at 333nm (Figure 7). The full-width at half maximum (FWHM) of peaks were 8.9nm for material grown on silicon, compared with 6.6nm for sapphire-based structures. The performance of the devices was somewhat similar.

The UV-LED from silicon-grown material achieved a maximum output power of 1.3mW at 700mA injection with 0.5% duty cycle and 10μs period (Figure 8). Although this represents only a 0.13% wall-plug efficiency, the result represents one of the highest values reported so far for silicon substrate growth at this wavelength. At higher duty cycles the peak power reduced, mostly likely due to thermal effects related to Shockley–Read–Hall recombination. Moving to continuous wave (CW) operation reduces the peak power by a factor of 300. For the LED grown on sapphire, the corresponding reduction factor was just 10.

Near-field analysis under the microscope showed defective current spreading in the LED grown on silicon, unlike the sapphire-based device. The researchers found cracks on the AlN surface where the silicon substrate was removed. The team comments: "Further investigations indicated that few AlN cracks were visible right after the growth (non-coalesced area or thermal cracking, for instance) and several ones were created during the device processing. Additionally, upon the substrate removal step, the acid mixture penetrated through the cracks and slightly etched the metal contacts and passivation layer of the LED/Si structure."

Further damage was caused by localized regions of high current density leading to hot spots and thermal instability at higher currents and duty cycles. The researchers believe that these factors explain the greater reduction in peak power in moving to CW operation from UV-LEDs grown on silicon. ∎

Author:
Mike Cooke is a freelance technology journalist who has worked in the semiconductor and advanced technology sectors since 1997.